ECCENTRICITY SAMPLES: IMPLICATIONS ON THE POTENTIAL AND THE VELOCITY DISTRIBUTION

R. Cubarsi[1], M. Stojanović[2] and S. Ninković[2]

[1]*Departament de Matemàtiques, Universitat Politècnica de Catalunya, Barcelona, Spain*

E–mail: *rafael.cubarsi@upc.edu*

[2]*Astronomical Observatory, Volgina 7, 11060 Belgrade 38, Serbia*

E–mail: *mstojanovic@aob.rs, sninkovic@aob.rs*

SUMMARY: Planar and vertical epicycle frequencies and local angular velocity are related to the derivatives up to the second order of the local potential and can be used to test the shape of the potential from stellar disc samples. These samples show a more complex velocity distribution than halo stars and should provide a more realistic test. We assume an axisymmetric potential allowing a mixture of independent ellipsoidal velocity distributions, of separable or Staeckel form in cylindrical or spherical coordinates. We prove that values of local constants are not consistent with a potential separable in addition in cylindrical coordinates and with a spherically symmetric potential. The simplest potential that fits the local constants is used to show that the harmonical and non-harmonical terms of the potential are equally important. The same analysis is used to estimate the local constants. Two families of nested subsamples selected for decreasing planar and vertical eccentricities are used to borne out the relation between the mean squared planar and vertical eccentricities and the velocity dispersions of the subsamples. According to the first-order epicycle model, the radial and vertical velocity components provide accurate information on the planar and vertical epicycle frequencies. However, it is impossible to account for the asymmetric drift which introduces a systematic bias in estimation of the third constant. Under a more general model, when the asymmetric drift is taken into account, the rotation velocity dispersions together with their asymmetric drift provide the correct fit for the local angular velocity. The consistency of the results shows that this new method based on the distribution of eccentricities is worth using for kinematic stellar samples.

Key words. Stars: kinematics – Galaxies: kinematics and dynamics – Galaxies: statistics – Galaxy: solar neighbourhood

1. INTRODUCTION

Several kinematic analyses suggest that the Galactic thin disc has a non-vanishing vertex deviation, the thick disc has a radial mean motion differing from that of the thin disc, and the halo velocity ellipsoid is likely to be tilted (Pasetto et al. 2012a,b,

Moni Bidin et al. 2012, Casetti-Dinescu et al. 2011, Carollo et al. 2010, Fuchs et al. 2009, Smith et al. 2009a,b, Siebert et al. 2008). What type of potentials allow to describe these kinematic features in the solar neighbourhood?

There is a large family of potentials consistent with one ellipsoidal stellar velocity distribution ac-

cording to Chandrasekhar's (1960) time dependent systems. For three-dimensional models these potentials were studied by Sala (1990). They include Eddington's (1915) and Lynden-Bell (1962) stationary potentials. However, for a mixture of stellar populations, by associating each stellar populations with an ellipsoidal velocity distribution, only few possible potentials remain. To determine which potentials are consistent with the integrability conditions imposed by a mixture of populations two approaches were made. In a first approach (Cubarsi 2014a), axisymmetric potentials satisfying the time-dependent colisionless Boltzmann equation (CBE) allowing a number of independent populations were studied. By independent populations we mean that they may have different mean velocities and arbitrary orientation of velocity ellipsoids.

In a Galactocentric cylindric coordinate system (r, θ, z), with θ positive in the direction of the Galactic rotation and z perpendicular to the Galactic plane and positive towards the NGP, the potential must have the form

$$\mathcal{U} = M\left(r^2 + z^2\right) + \frac{1}{r^2}F(z^2/r^2) , \qquad (1)$$

where F is an arbitrary function of its argument $s = z^2/r^2$ (or of the polar angle $\varphi = \arctan\sqrt{s}$). It is an axisymmetric potential of Stäckel form in cylindrical and spherical coordinates. If the potential is stationary then M is constant, otherwise it is the only part of the potential that may depend on time-dependent kinematic parameters. For this reason it was called quasi-stationary potential.

Since Pasetto et al. (2012b) and Steinmetz (2012) had suggested that the axisymmetry assumption should be relaxed towards a model with point-axial symmetry in order to account for such a kinematic features, in a second approach (Cubarsi 2014b) the point-asymmetric model i.e. rotational symmetry of $180°$ for the potential and the phase space density functions, was studied. The result was that the potential had to be also axisymmetric and, in particular, spherical, according to:

$$\mathcal{U} = M\left(r^2 + z^2\right) + \frac{N}{r^2 + z^2} . \qquad (2)$$

However, such a spherical potential did not allow for either vertex deviation of the population velocity ellipsoids in the Galactic plane or tilt of the ellipsoids out of the Galactic plane.

However, the apparent vertex deviation of disc samples could also be produced, at least from a strictly mathematical point of view, from a mixture of several populations having different radial and rotation mean velocities, each one without vertex deviation or even spheroidal. On the other hand, as Smith et al. (2009a) suggested, the tilted velocity ellipsoids of the thick disc and halo could be the result of stellar samples not sufficiently mixed in order

to produce well defined velocity ellipsoids or of samples contaminated by disc stars. Similarly, Evans et al. (2016) argue that a spherical potential is consistent with the velocity distribution of halo stellar samples. But halo stars are not expected to show the complexity of disc stellar samples.

Therefore, the shape or the symmetry of the potential should be justified from other and better reasons, if possible from disc stellar samples. The main purpose of the current study is to test the consistency of the potential in the general form of Eq. (1) against the local velocity distribution, in particular, the velocity dispersions and the asymmetric drift of the samples. Thus, we shall focus on the main trends of the disc stars which involve the local kinematic constants, namely the planar and vertical epicycle frequencies, and the local angular velocity.

Under the first-order epicycle model, for a given stellar sample the epicycle frequencies are related to the second velocity central moments[1] μ_{rr} and μ_{zz} through the mean squared planar and vertical star eccentricities. This model, however, is unable to provide a realistic value of the local angular velocity from a similar relationship between the moment $\mu_{\theta\theta}$ and the mean squared planar eccentricity. This will be addressed by leaving aside the epicycle model and by taking into account the asymmetric drift of the samples.

In Cubarsi (2010) it was proved that, in order to obtain kinematically three-dimensional velocity stellar samples kinematically of the Galactic disc, the orbital eccentricity behaves as an excellent sampling parameter which allows to distinguish a number of small-scale features of the velocity distribution. Instead, other sampling parameters such as the absolute value of the heliocentric velocity, metalicity [Fe/H], or colour $b - y$, produce kinematically biased samples and population estimates if they are not complemented with other sampling criteria such as the limit of the absolute space motion. In particular, by using the stars of the Geneva-Copenhagen Survey II (Nordström et al. 2004, Holmberg et al. 2007) which include star's eccentricities, maximum planar eccentricity $e = 0.3$ and maximum distance to the Galactic plane $z_{\max} = 0.5$ kpc led to a kinematically representative sample of the thin disc. Therefore, the purpose of the current work is to use, along with star's velocities, the eccentricity distribution to study the potential and the velocity distribution.

The planar and vertical eccentricities e and e_z, according to the generalised notion of Ninković (2009), are related to the star's orbit and can be computed by using approximations concerning the gravitational potential (Ninković 2011). At a distance r_0 from the Galactic centre (GC), $z_{\max}$ and the vertical eccentricity e_z are proportional: $z_{\max} = r_0 e_z$. When these data are available, their use as sampling parameters provides velocity samples far more representative of the moving groups they contain than if the samples had been selected by the absolute space motion. In order to draw several nested subsamples of the disc and to compute the mean squared eccen-

---

[1] The central moments are here expressed in the component notation, according to the mean value $\mu_{i_1 i_2 \ldots i_n} = \langle u_{i_1} u_{i_2} \ldots u_{i_n} \rangle$ with indices in the set $\{1, 2, 3\}$, depending on the peculiar velocity component.

tricities and the second velocity central moments, we shall use the updated Geneva-Copenhagen Survey III (hereafter GCSIII) catalogue (Holmberg et al. 2009).

The first step is to describe how the local constants and the potential are related. A first approach for disc stars involves the use of the epicycle approximation in order to model the distribution of star eccentricities. Although this is a classical astronomical topic (e.g. Binney and Tremaine 2008), we shall detail it in order to introduce notation and definitions. In addition, the referred book does not take into account the eccentricity distribution when studying the epicycle approximation. The local kinematic properties are afterwards referred to the comoving reference frame, for which we are able to get the kinematic estimates.

A second step consists in study of how the velocity distribution and eccentricities are related. We analyse how these relationships constrain the ratios of the semiaxes of the velocity ellipsoids. Now, it is necessary to adopt a more general approach than the epicycle model in order to consider the asymmetric drift of stellar samples. This approach is studied for the general case where the three mean velocity components of a stellar population may differ from the circular velocity orbit.

In a third step we obtain the local Galactic constants from nested stellar samples selected by planar and vertical eccentricities. The planar epicycle frequency is easily deduced from nested stellar subsamples selected by planar eccentricity. The vertical epicycle frequency is straightforward obtained from nested stellar subsamples selected by maximum height. Nested stellar subsamples selected by planar eccentricity should also provide a good estimation of the local angular velocity. However, this does not occur since the first order epicycle model neglects the asymmetric drift. When this term is taken into account, the local angular velocity is correctly estimated as well. This approach leads to a simple way for evaluating the asymmetric drift from the second velocity central moments.

Finally, we discuss the implications that the actual values of local kinematical constants have on the shape of the potential. By assuming the above family of potentials allowing mixtures of independent ellipsoidal velocity distributions, we prove that the potential cannot be separable in addition in cylindrical coordinates and cannot be spherically symmetric.

2. LOCAL KINEMATICAL CONSTANTS

The solution of the equations of motion of a point mass particle under a conservative force field is constrained by the knowledge about the potential function. In the Galaxy, the mutual gravitational interactions of the stars determine their orbits. Leaving aside stellar encounters, these interactions arise from the smoothed-out stellar distribution of matter, which is given through a quite unknown gravitational potential. However, some symmetry properties may be generally assumed providing us with a basic set of integrals of motion. The epicycle approximation is a particular case of integration of the equations of motion under a minimum set of hypotheses allowing to

obtain solutions for nearly circular orbits in the three dimensional space. Although it is described in many standard books on astronomy, in order to fix the notation, we explain the method from scratch by determining the solution for circular orbits in Appendix A (Epicycle approximation). Under this approach, the orbit of any star projected onto the Galactic plane describes an ellipse with origin at a guiding centre or epicentre which moves uniformly in a circular orbit around the GC. The model leads to interesting properties about the star motion, such as the planar and vertical epicycle frequencies, and the axial ratio of the planar epicycle, which only depend on local properties of the potential, as well as properties about the local stellar velocity distribution and their relation to some eccentricity statistics.

Linblad's approach consists in to refer the orbit of a star with position (r, θ, z) near the Galactic plane to a reference frame with centre in the position $(r_c, \theta_c, 0)$ of a star in the Galactic plane in circular motion *with the same angular momentum integral J_c*. It is the guiding centre C for which, given the position and velocity of a star, we may obtain r_c and Ω_c which satisfy Eqs. (87) and (90).

For the first two coordinates, we may write

$$r = r_c + \varepsilon; \quad \theta = \theta_c + \delta . \qquad (3)$$

The first requirement for the validity of the model is

$$\varepsilon \ll r_c . \qquad (4)$$

The second, since θ_c may have an arbitrary origin, by differentiating Eq. (3) we get

$$\dot{r} = \dot{\varepsilon}; \quad \dot{\theta} = \Omega_c + \dot{\delta} , \qquad (5)$$

and we assume

$$|\dot{\delta}| \ll |\Omega_c| . \qquad (6)$$

The values ε and $\dot{\delta}$ are constrained since the angular momentum integral is fixed. Thus, by taking into account Eq. (79), Eq. (3), and Eq. (5) we have

$$\begin{aligned} J_c &= (\Omega_c + \dot{\delta})(r_c + \varepsilon)^2 \\ &= \Omega_c r_c^2 + 2\Omega_c r_c \varepsilon + r_c^2 \dot{\delta} + \Omega_c \varepsilon^2 + 2r_c \varepsilon \dot{\delta} + \varepsilon^2 \dot{\delta} . \end{aligned}$$

Being $J_c = \Omega_c r_c^2$, by considering only the terms up to first order, we get

$$2\Omega_c r_c \varepsilon + r_c^2 \dot{\delta} = 0 .$$

Therefore, we get the relationship

$$\dot{\delta} = -\frac{2\Omega_c}{r_c} \varepsilon . \qquad (7)$$

Notice that, if $\Omega_c > 0$ then $\dot{\delta}$ and ε have opposite signs, as shown in Fig. 1.

To obtain the orbit of the star in the circular motion reference frame we write the first equation of motion in Eq. (76) in terms of the *effective potential energy* gradient, defined in Eq. (85), so that

$$\ddot{r} = -\frac{\partial \mathcal{V}}{\partial r} \; , \qquad (8)$$

and we expand it up to the first order around the guiding centre C

$$\frac{\partial \mathcal{V}}{\partial r} \approx \left.\frac{\partial \mathcal{V}}{\partial r}\right|_{c} + \left.\frac{\partial^2 \mathcal{V}}{\partial r^2}\right|_{c} \varepsilon \; .$$

The first term, according to Eq. (86), is null, and the second term, according to Eq. (88), is

$$\kappa^2 = \left.\frac{\partial^2 \mathcal{V}}{\partial r^2}\right|_{c} \; . \qquad (9)$$

Then, from Eq. (3) the radial component of the equations of motion becomes

$$\ddot{\varepsilon} = -\kappa^2 \varepsilon \; . \qquad (10)$$

Therefore, the condition of a local minimum of the effective potential energy at r_c, given by Eq. (84), ensures the orbit to be stable.

The approximation given by Eq. (10) describes the radial motion of the star as an harmonic oscillator around the guiding centre C with frequency κ

$$\varepsilon = a \, \sin(\kappa t - p) \; . \qquad (11)$$

The positive value of κ is the *planar epicycle frequency*, and a and p are integration constants.

The axial component is easily obtained by integrating Eq. (7),

$$\dot{\delta} = -\frac{2\Omega_c}{r_c} a \, \sin(\kappa t - p) \; , \qquad (12)$$

$$\delta = \frac{2\Omega_c}{r_c \, \kappa} a \, \cos(\kappa t - p) \; , \qquad (13)$$

where the additive integration constant can be assumed as null since $\varepsilon \to 0$ and $\delta \to 0$ when $a \to 0$.

In a similar way, the vertical component z of the star referred to the guiding centre C in the Galactic plane is obtained in a first order approximation by expanding the vertical gradient of the potential as

$$\frac{\partial \mathcal{U}}{\partial z} \approx \left.\frac{\partial^2 \mathcal{U}}{\partial z^2}\right|_{c} z \; ,$$

so that we obtain

$$z = b \, \sin(\nu t - q) \; , \qquad (14)$$

being

$$\nu^2 = \left.\frac{\partial^2 \mathcal{U}}{\partial z^2}\right|_{c} > 0 \; , \qquad (15)$$

where ν is the *vertical epicycle frequency*, and b and q integration constants. Usually, the constant b is notated as the star's maximum height z_{max}.

2.1. Position referred to the circular orbit

A star at a position S, with coordinates (x, y, z) referred to the GC, will be referred to the circular velocity of the guiding centre C in the Galactic plane with coordinates $(r_c, \theta_c, 0)$ which is moving with circular velocity $\Theta_c = \Omega_c r_c$ (see Fig. 1). Then, the new Cartesian coordinates (ξ, η, ζ) of the star satisfy:

$$\xi = \varepsilon = a \, \sin(\kappa t - p) \; ,$$

$$\eta = r_c \, \delta = \tfrac{2\Omega_c}{\kappa} a \, \cos(\kappa t - p) \; , \qquad (16)$$

$$\zeta = z = b \, \sin(\nu t - q) \; .$$

We focus on the star's motion projected onto the Galactic plane since the motion in the direction ζ is independent of the other coordinates. Vertically, the star simply oscillates about the Galactic plane. For a simpler notation we use the dimensionless constant

$$\gamma_c = \frac{2\Omega_c}{\kappa} \; , \qquad (17)$$

depending on the local values of the star and the potential. It is not, strictly speaking, a new constant. Then, the coordinates (ξ, η) describe the following ellipse centred at C

$$\xi^2 + \gamma_c^{-2}\eta^2 = a^2 \qquad (18)$$

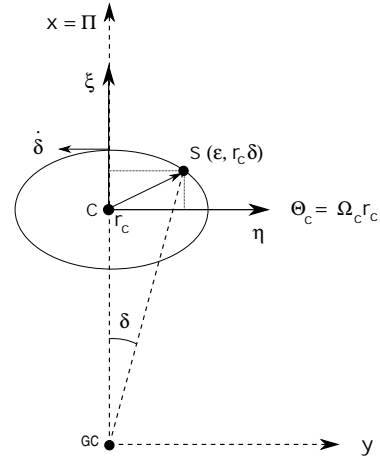where γ_c^{-1} is the ratio of axes.

Fig. 1. *In the Galactic plane, the star S is referred to the GC with coordinates (x, y) and to the circular velocity of the guiding centre C, with circular velocity $\Theta_c = \Omega_c r_c$, with coordinates (ξ, η).*

Notice that the local velocities, being referred to C, describe an ellipse with the same axis ratio than the previous one,

$$\dot{\xi} = a\kappa \, \cos(\kappa t - p) = \kappa \gamma_c^{-1} \eta \; ,$$

$$\dot{\eta} = -2\Omega_c a \, \sin(\kappa t - p) = -2\Omega_c \xi \; , \qquad (19)$$

$$\dot{\zeta} = \nu b \, \cos(\nu t - q) \; .$$

Hence, it is fulfilled

$$\dot{\xi}^2 + \gamma_c^{-2}\dot{\eta}^2 = \kappa^2 a^2 \ . \qquad (20)$$

It is worth noticing that above ellipses are relative to the guiding centre C, which is specific of each star.

Finally, the motion of the star referred to the GC is easily obtained in cylindrical coordinates according to

$$r = r_c + \varepsilon = r_c + a\,\sin(\kappa t - p) \ ,$$

$$\theta = \theta_c + \delta = \theta_0 + \Omega_c\,t + \frac{\gamma_c\,a}{r_c}\,\cos(\kappa t - p) \ , \qquad (21)$$

$$z = b\,\sin(\nu t - q) \ .$$

3. POTENTIAL

In the past section we have shown that the radial and transversal epicycle frequencies are the same and, like the vertical frequency, they are constant, not depending on the star but on local values of the potential. This is an important result obtained in the twenties by Oort and Lindblad. Each region in a galaxy provides stars with a local oscillation mode. As we have adopted an axisymmetric model, the epicycle frequencies would vary depending on the distance to the GC and to the plane. First we study the implications on the potential, and afterwards we shall estimate how much the epicycle frequencies may vary from one point to another.

We shall assume a quasi-stationary potential given by Eq. (1), i.e. an axisymmetric potential allowing for finite mixture of ellipsoidal velocity distributions and, in addition, arbitrary population mean velocities in the radial, rotation, and vertical components (although in the symmetry plane the vertical mean velocity is null). This potential satisfies the time-dependent CBE for axially symmetric stellar systems. The particular case of a spherical potential is the solution of the CBE for stellar system with point-to-point axial symmetry (Cubarsi 2014b). Let us remember that a stationary potential does not imply a steady-state stellar system, that is, a stationary velocity distribution. Indeed, a time dependent velocity distribution is needed to allow for a non-vanishing radial mean velocity of the stellar populations.

It is worth noticing that, for steady-state stellar systems, the potential allowing the alignment of the stress tensor along an orthogonal coordinate system is of separable or Stäckel form (An and Evans 2016, Evans et al. 2016). These authors suggest that the actual case should be very close to the spherical alignment and they obtain a potential similar to that of Eq. (1) where the first term, instead of the harmonic potential, is an arbitrary function of $r^2 + z^2$. In our case, where each population velocity distribution is ellipsoidal in the peculiar velocities, this term becomes totally determined since this is the only possibilty allowing differential radial motion of populations.

In particular, to study the spherical case, Eq. (1) can also be written as

$$\mathcal{U} = M\,(r^2 + z^2) + \frac{1}{r^2 + z^2}\,N(z^2/r^2) \ , \qquad (22)$$

where

$$F(z^2/r^2) = N(z^2/r^2)\,\left(1 + \frac{z^2}{r^2}\right)^{-1} \ .$$

In addition to the general case, we shall study two particular cases. One with constant F in Eq. (1), corresponding to a potential separable in addition in cylindrical coordinates, and another one with constant N in Eq. (22), corresponding to the spherical potential.

3.1. Separable cylindrical potential

We assume the potential of Eq. (1) separable in addition in cylindrical coordinates

$$\mathcal{U} = M\,(r^2 + z^2) + \frac{F}{r^2} \ . \qquad (23)$$

where F is constant.

We define the following linear operator, which appeared in the condition of orbital stability of Eq. (88), acting over the potential $\mathcal{U}$

$$L_r[\cdot] = \left(\frac{\partial^2}{\partial r^2} + \frac{3}{r}\frac{\partial}{\partial r}\right)[\cdot] \ . \qquad (24)$$

It satisfies $L_r[c_1\,r^{-2} + c_2] = 0$ either with c_1, c_2 constants or functions of z. Furthermore,

$$L_r[Mr^2] = 8M \ .$$

Then, these potentials provide constant squared epicycle frequencies $\kappa^2 = 8M$ and, according to Eq. (15), $\nu^2 = 2M$ regardless the point in the Galaxy.

Therefore, on one hand, the existence of bounded orbits requires the factor M to be positive. On the other hand, the constant M determines both epicycle frequencies. Then, the ratio of the epicycle frequencies is $\frac{\kappa}{\nu} = 2$, which is not the actual case, since, according to the commonly accepted values $\Omega_c \approx 27$ km s^{-1}kpc^{-1}, $\kappa \approx 37$ km s^{-1}kpc^{-1}, and $\nu \approx 70$ km s^{-1}kpc^{-1} (e.g. Binney and Tremaine 2008, Table 1.2), the vertical frequency must be higher than the planar (the rotation period is about 220 Myr and the vertical period of oscillation is approximately 87 Myr).

By Eq. (87), in the Galactic plane, for a star in circular motion and angular momentum integral J, the radius r_c of the circular orbit verifies

$$r_c^4 = \frac{2F + J^2}{2M} \ .$$

Since $M > 0$, then $J^2 > -2F$. This is the condition for a stable orbit. Thus, a repulsive force associated with the potential term with $F > 0$ would allow stable orbits for all the stars. This excludes the existence of circular orbits within a radius lower that $r_{\min} = [F/M]^{\frac{1}{4}}$, corresponding to the value $J = 0$.

Otherwise, an attractive force associated with $F < 0$ would allow bounded orbits at any distance from the GC but only for stars trespassing a threshold angular velocity with a minimum angular momentum integral $J_{\min}^2 = -2F$. Other orbits become unstable.

The angular velocity satisfies Eq. (90). Then, for the potential in Eq. (1), the squared angular velocity in terms of the radius of any star in a circular orbit on the Galactic plane is given by

$$\Omega_c^2(r) = 2M - \frac{2F}{r^4}, \quad r^4 \geq F/M \ . \qquad (25)$$

By expressing M in terms of the planar epicycle frequency, for $r = r_c$ we determine F from the local angular velocity, i.e.

$$F = \frac{r_c^4}{2}\left(\frac{\kappa^2}{4} - \Omega_c^2(r_c)\right) \ . \qquad (26)$$

The local values for these constants allow estimates $\frac{\kappa^2}{4} \approx 340$ and $\Omega_c^2(r_c) \approx 730$ (both values in km^2 s^{-2}kpc^{-2}).

Then, for such a potential, F is negative. Therefore, an attractive force requires $\kappa < 2\Omega_c$.

3.2. Spherical potential

We assume the spherical potential of Eq. (22) with constant N, that is, Eq. (2). In the symmetry plane, the planar epicycle frequency is, like in the previous case, constant $\kappa^2 = 8M$.

On the other hand, the vertical epicycle frequency at $z = 0$ is

$$\nu^2 = \left.\frac{\partial^2 \mathcal{U}}{\partial z^2}\right|_c = 2M - \frac{2N}{r_c^4} \ . \qquad (27)$$

Then, in the Galactic plane both epicycle frequencies are constrained according to the relationship

$$N = \frac{r_c^4}{2}\left(\frac{\kappa^2}{4} - \nu^2\right) \ . \qquad (28)$$

Hence, N is now related to the local vertical epicycle frequency. Since the actual values in the solar neighbourhood satisfy $\nu > \kappa$, the above equation would provide a negative value for the constant N. Similarly, an attractive force requires $\kappa < 2\nu$.

However, by comparing Eq. (25) and Eq. (27), since the spherical and separable cylindrical potentials satisfy $F = N$ and $\kappa^2 = 8M$, we get

$$\nu^2 = \Omega_c^2(r_c) \ .$$

Therefore, for the spherical potential in the Galactic plane, the local vertical epicycle frequency and the

absolute value of the local angular velocity match at r_c. There is no alternative parameter to fit the local angular velocity. This could neither be the actual case in the solar neighbourhood.

3.3. General case

For the general case of Eq. (1), according to the term having the arbitrary function $F(s)$ with $s = z^2/r^2$, we get

$$L_r[\mathcal{U}] = 8M + \frac{1}{r^4}\left(8sF'(s) + 4s^2F''(s)\right) \qquad (29)$$

and

$$\frac{\partial^2 \mathcal{U}}{\partial z^2} = 2M + \frac{1}{r^4}\left(2F'(s) + 4sF''(s)\right) \ . \qquad (30)$$

Then, in the Galactic plane, $s = 0$, the epicycle frequencies satisfy

$$\kappa^2 = 8M, \quad \nu^2 - \frac{\kappa^2}{4} = \frac{2F'(0)}{r_c^4} \ . \qquad (31)$$

In addition, Eq. (25) becomes

$$\Omega_c^2(r_c) - \frac{\kappa^2}{4} = -\frac{2F(0)}{r_c^4} \ . \qquad (32)$$

For the second term of potential (23), an attractive force in terms of r and $|z|$ is associated with local values $F(0) < 0$ and $F'(0) > 0$. Therefore, it implies $2\Omega_c > \kappa$ and $2\nu > \kappa$. Then, such a potential term increases the force produced by the harmonic potential.

Therefore, we have three independent parameters related to the three local constants. They can be adjusted according to actual values and provide the local derivatives of the potential function

$$\begin{aligned}
\left.\frac{\partial \mathcal{U}}{\partial r}\right|_{(r_c,0)} &= \Omega_c^2 r_c \ , \\
\left.\frac{\partial^2 \mathcal{U}}{\partial r^2}\right|_{(r_c,0)} &= \kappa^2 - 3\Omega_c^2 \ , \\
\left.\frac{\partial^2 \mathcal{U}}{\partial z^2}\right|_{(r_c,0)} &= \nu^2 \ .
\end{aligned} \qquad (33)$$

4. KINEMATICS

We compare two close circular orbits at radii $r = r_c$ and $r = r_c + \varepsilon$ in the Galactic plane. Each characteristic angular velocity $\Omega_c(r)$ is given by Eq. (90). The corresponding angular momentum $J_c(r)$ of a star in circular orbit at a radius r is equal to $r^2\Omega_c(r)$. By taking into account the first equation of

motion in Eq. (76), we may determine how the angular velocity, the circular velocity, and the angular momentum integral vary from one circular orbit to another. For a given potential, the circular velocity Θ_c at a radius r satisfies

$$\frac{\Theta_c^2(r)}{r} = \frac{\partial \mathcal{U}(r,0)}{\partial r} , \qquad (34)$$

and its derivative is:

$$\frac{2\Theta_c(r)}{r}\frac{\partial \Theta_c(r)}{\partial r} - \frac{\Theta_c^2(r)}{r^2} = \frac{\partial^2 \mathcal{U}(r,0)}{\partial r^2} . \qquad (35)$$

The above equations allow us to obtain the planar epicycle frequency at $r = r_c$ in terms of the local circular velocity and its derivative, instead of in terms of the potential derivatives, so that

$$\kappa^2 = \frac{2\Theta_c(r_c)}{r_c}\left(\frac{\Theta_c(r_c)}{r_c} + \frac{\partial \Theta_c(r)}{\partial r}\bigg|_{r_c}\right) . \qquad (36)$$

Conversely, from Eq. (36) we can estimate the first derivative of the circular velocity at r_c in terms of the local epicycle frequency, which is easily written by using the angular velocity $\Omega = \Theta/r$

$$\frac{\partial \Theta_c(r)}{\partial r}\bigg|_{r_c} = \frac{\kappa^2}{2\Omega_c(r_c)} - \Omega_c(r_c) . \qquad (37)$$

Therefore, in a first order approximation, and by taking into account the definition of γ_c in Eq. (17), the circular velocity $\Theta_c(r_c + \varepsilon)$ may be estimated as

$$\Theta_c(r_c + \varepsilon) = \Theta_c(r_c) + \left(\kappa\gamma_c^{-1} - \Omega_c(r_c)\right)\varepsilon . \qquad (38)$$

By working in a similar way, we can write the following radial gradients

$$\frac{\partial \Omega_c(r)}{\partial r}\bigg|_{r_c} = \frac{\kappa\gamma_c^{-1} - 2\Omega_c(r_c)}{r_c}, \qquad (39)$$

$$\frac{\partial J_c(r)}{\partial r}\bigg|_{r_c} = \kappa\gamma_c^{-1}r_c . \qquad (40)$$

Notice that the approximation:

$$\Omega_c(r_c + \varepsilon) = \Omega_c(r_c) + \left(\kappa\gamma_c^{-1} - 2\Omega_c(r_c)\right)\frac{\varepsilon}{r_c} , \qquad (41)$$

being $\varepsilon \ll r_c$, allows us to assume a nearly constant angular circular velocity for all circular orbits around the radius r_c.

Then, for sufficiently large values of r_c, the assumption that the angular velocity $\Omega_c(r_c)$ is nearly constant around r_c is much more accurate than for $\Theta_c(r_c)$.

4.1. Comoving reference frame

We wish to refer the velocity of a star passing through the point S, having coordinates (ξ, η, ζ) with respect to the circular orbit centred in C, to the circular orbit centred in a fixed point S_0, which is the projection of S onto the plane $z = 0$, with coordinates $(\xi, \eta, 0)$. Therefore, the angular momentum integral of the orbits passing through C and S are the same, while the one of the circular orbit in S_0, according to Eq. (40), differs by the amount $\frac{\partial J_c(r)}{\partial r}\big|_{r_c}\xi$.

There is no radial motion in both circular orbits so that $\Pi_c \equiv \Pi_c(C) = 0$ and $\Pi_c(S_0) = 0$. Hence, the Galactocentric radial velocity of the star, as well as the radial velocity referred to the circular orbit, is $\Pi = \dot{\xi}$. Thus, by Eqs. (17) and (19), we may write

$$\Pi(S) - \Pi_c(S_0) = \kappa\gamma_c^{-1}\eta = \kappa a \cos(\kappa t - p) . \qquad (42)$$

Similarly, there is is no vertical motion in both circular orbits in the Galactic plane, so that $Z_c \equiv Z_c(C) = 0$ and $Z_c(S_0) = 0$. Then, the vertical velocity of the star satisfies $Z = \dot{\zeta}$, which we write as

$$Z(S) - Z_c(S_0) = \nu b \cos(\nu t - q) . \qquad (43)$$

On the other hand, for the velocity component of the star along Galactic roation, bearing in mind Eq. (3) and the equivalence $\xi = \varepsilon$, we have

$$\Theta(S) = (r_c + \xi)(\Omega_c(C) + \dot{\delta})$$
$$= \Omega_c(C)\,r_c + r_c\dot{\delta} + \Omega_c(C)\,\xi + \xi\dot{\delta} .$$

We only consider up to the first order terms and take into account Eq. (7). Thus

$$\Theta(S) = \Omega_c(C)\,r_c - \Omega_c(C)\,\xi = \Theta_c(C) - \Omega_c(C)\,\xi. \qquad (44)$$

Also, according to Eq. (38), the circular velocity at S_0 may be approximated from the circular orbit at C as

$$\Theta_c(S_0) = \Theta_c(C) + \left(\kappa\gamma_c^{-1} - \Omega_c(C)\right)\xi . \qquad (45)$$

Therefore, by subtraction of Eq. (45) from Eq. (44) and using Eqs. (16), we get

$$\Theta(S) - \Theta_c(S_0) = -\kappa\gamma_c^{-1}\xi = -\kappa\gamma_c^{-1}a\sin(\kappa t - p) . \qquad (46)$$

Finally, by substitution of ξ and η from Eqs. (42) and (44) into Eq. (18), we get

$$[\Pi - \Pi_c(S_0)]^2 + \gamma_c^2\,[\Theta - \Theta_c(S_0)]^2 = \kappa^2 a^2 . \qquad (47)$$

This is the equation for a family of ellipses centred at the planar circular velocity in S_0, whose semiaxes are in inverse proportion with regard to the ellipses of Eq. (18) and Eq. (20). While the latter ellipses are centred at a different guiding centre C for each star, the family of Eq. (47) has a common centre at S_0 for all the stars passing through S and, in general, due to the axial symmetry and to the symmetry plane, for all the stars with the same coordinates (r, θ). In

addition, we may assume that κ and γ_c are similar at the points C, S_0, and S.

Notice that the values κ and γ_c in Eq. (17) depend on Ω_c, which is nearly constant around C as deduced from Eq. (41). However, the epicycle model introduces a larger error in assuming a similar value for Θ_c at C, S_0, and S.

Usually the local parameters κ and γ_c are expressed in terms of the Oort constants, A and B, of the field of differential motions at the point S_0 in the Galactic plane, as described in Appendix B (Oort constants).

5. VELOCITY STATISTICS

For a fixed time t, we wish to calculate some velocity statistics for a local sample composed of stars around the point S in order to estimate the local values κ, ν, and γ_c. In this process the variables involved are those of Eqs. (42), (46) and (43), namely, the velocity components (Π, Θ, Z), the star amplitudes a and b, and the phases p and q.

In particular, the values a and b are related to the planar and vertical eccentricities. The planar eccentricity is a dimensionless measure of deviation from circular motion in the Galactic plane, defined as

$$e = \frac{r_a - r_p}{2r_0} , \qquad (48)$$

where r_a and r_p are the extremal distances to the rotation axis, and

$$r_0 = \frac{r_a + r_p}{2} , \qquad (49)$$

is their arithmetic mean. We assume $r_0 = r_c$. Therefore, the amplitude a of Eq. (16) corresponds to $\frac{r_a - r_p}{2}$, and the planar eccentricity is

$$e = \frac{a}{r_0} . \qquad (50)$$

On the other hand, the vertical eccentricity is defined as

$$e_z = \frac{1}{2} \frac{|z_a| + |z_p|}{r_0} \qquad (51)$$

where $|z_a|$ and $|z_p|$ are the amplitudes of the distances to the Galactic plane. For stars about the Galactic plane, the amplitude $b \equiv z_{max}$ in Eq. (14) is the same as $\frac{|z_a| + |z_p|}{2}$. Then, the vertical eccentricity satisfies

$$e_z = \frac{z_{max}}{r_0} . \qquad (52)$$

The velocity variables have a trivariate distribution that, for large stellar samples, may be managed as a Gaussian population mixture. A priori it is not easy to select a stellar sample containing a single population since the sampling parameters always produce truncated or overlapped velocity distributions. The eccentricity e and the planar amplitude

40

$a = e\, r_0$ are random variables that, for large disc samples, have an approximate lognormal distribution (Cubarsi 2010). The distance r_0 to the GC may be assumed the same for all stars of a local sample. The maximum height z_{max} behaves like the planar amplitude. Since the vertical and planar motions were solved separately, they involve independent random variables. The planar and vertical phases p, q, with no prior information about them, taken for granted that the stars are well mixed, may be reasonably assumed as uniformly distributed in $[-\pi, \pi]$. Furthermore, phases and eccentricities are independent variables, since they are the two integration constants of the second-order differential equation governing the star's motion.

In Cubarsi (2010) the eccentricity was proven a very useful sampling parameter in order to isolate particular kinematic behaviours of thin disc subsamples. Both planar and vertical amplitudes have to be combined in order to exclude thick disc or halo stars. Several nested stellar samples selected as increasing the star eccentricity did provide a very detailed representation of the small and large scale kinematic structure of local stars associated with the main moving groups. It could be said that the eccentricity is a highly respectful sampling parameter of kinematically homogeneous stars. Now, we will deepen in the kinematic information provided by the eccentricities.

5.1. Stars in nearly circular orbits

For fixed time and position, the characteristic circular motion values κ, ν, γ_c are constant. We calculate the expected values $E(\cdot) \equiv \langle \cdot \rangle$ of the stars in a sample Σ for the above mentioned random variables. The sample Σ will be chosen to have maximum eccentricity

$$e_0 = \max_{e \in \Sigma}(e) ,$$

and maximum height

$$z_0 = \max_{z_{max} \in \Sigma}(z_{max}) .$$

Moreover, this will be done for a series of subsamples in order to study the main trends and stability of the estimates. For a sample $\Sigma(e_0)$ selected by planar eccentricity, the mean values $E(e)$ and $E(e^2)$ are increasing functions of e_0. Similarly, for of a sample $\Sigma(z_0)$ selected by the star height, the mean values $E(z_{max})$ and $E(z_{max}^2)$ are increasing functions of z_0, as shown in Fig. 4.

By taking expected values in the Eqs. (42) and (46), we get

$$\langle \Pi \rangle - \Pi_c(S_0) = \kappa \langle a \rangle \langle \cos(\kappa t - p) \rangle ,$$
$$\langle \Theta \rangle - \Theta_c(S_0) = -\kappa \gamma_c^{-1} \langle a \rangle \langle \sin(\kappa t - p) \rangle . \qquad (53)$$

If we write the mean velocity components at S as $\Pi_0 = \langle \Pi \rangle$ and $\Theta_0 = \langle \Theta \rangle$, since $\Pi_c(S_0) = 0$ and

$$\langle \cos(\kappa t - p) \rangle = \langle \sin(\kappa t - p) \rangle = 0 , \qquad (54)$$

then, the epicycle model provides a local centroid at S with velocities

$$\Pi_0 = \Pi_c(S_0) = 0, \quad \Theta_0 = \Theta_c(S_0) . \qquad (55)$$

Therefore, such a first-order epicycle model *cannot give an account for the asymmetric drift* i.e. the difference between the local circular velocity at S_0 and the local mean rotation velocity at S of the stellar population composing the sample Σ,

$$\Delta \equiv \Delta_\theta = \Theta_c(S_0) - \Theta_0(S_0) . \qquad (56)$$

This is one of the main limitations of the epicycle model.

We now compute the velocity variances i.e. the diagonal second central moments, from Eqs. (42) and (46). Since $\Pi_c(S_0)$ and $\Theta_c(S_0)$ are constants, we have

$$\mu_{rr} \equiv V[\Pi] = V[\Pi - \Pi_c(S_0)] ,$$
$$\mu_{\theta\theta} \equiv V[\Theta] = V[\Theta - \Theta_c(S_0)] . \qquad (57)$$

Bearing in mind Eq. (54), as well as the independence of the variables a and p, we then obtain

$$\mu_{rr} = \langle [\kappa a \cos(\kappa t - p)]^2 \rangle - \langle \kappa a \cos(\kappa t - p) \rangle^2$$
$$= \kappa^2 \langle a^2 \rangle \langle \cos^2(\kappa t - p) \rangle$$

and, similarly

$$\mu_{\theta\theta} = \langle [\kappa \gamma_c^{-1} a \sin(\kappa t - p)]^2 \rangle - \langle \kappa \gamma_c^{-1} a \sin(\kappa t - p) \rangle^2$$
$$= \kappa^2 \gamma_c^{-2} \langle a^2 \rangle \langle \sin^2(\kappa t - p) \rangle .$$

It is easy to see that the uniform distribution of p leads to

$$\langle \cos^2(\kappa t - p) \rangle = \langle \sin^2(\kappa t - p) \rangle = \frac{1}{2} . \qquad (58)$$

Thus, the relationships between the second velocity central moments and the mean value of the squared planar amplitude of a sample Σ are given by

$$\mu_{rr} = \frac{1}{2} \kappa^2 \langle a^2 \rangle ,$$
$$\mu_{\theta\theta} = \frac{1}{2} \kappa^2 \gamma_c^{-2} \langle a^2 \rangle . \qquad (59)$$

Let us remark that the expected value

$$\langle a^2 \rangle = r_0^2 \langle e^2 \rangle$$

is not proportional to the square of the average eccentricity of the sample $\langle a \rangle^2$ as it could be misinterpreted from Binney and Tremaine (2008, p170, equations 3.97 and 3.99). Since they do not take into account the eccentricity distribution i.e. they do not consider the eccentricity as a random variable and use X for $\langle a \rangle$ and X^2 for $\langle a^2 \rangle$, which is not correct.

By adding the expressions of Eq. (59), we get

$$\mu_{rr} + \gamma_c^2 \mu_{\theta\theta} = \kappa^2 \langle a^2 \rangle . \qquad (60)$$

Therefore, according to the epicycle model, the ratio of variances is

$$\frac{\mu_{rr}}{\mu_{\theta\theta}} = \gamma_c^2 , \qquad (61)$$

which is a value depending on the local properties of the stellar system, but not depending on the average values of the eccentricities of the sample.

However, this is not exact, as we shall see in the numerical application. If the model accounts for the asymmetric drift, we will get a more accurate relationship as explained in the next Section.

For the vertical motion, a similar reasoning for the epicycle approximation leads to $Z_0 = Z_c(S_0) = 0$. Then, since

$$\mu_{zz} \equiv V[Z] = V[Z - Z_c(S_0)] ,$$

we get from Eq. (43) the relationship between the second central moment μ_{zz} and the mean value of the squared vertical amplitude:

$$\mu_{zz} = \frac{1}{2} \nu^2 \langle z_{\max}^2 \rangle . \qquad (62)$$

Thus, the moments of such a sample satisfy

$$\frac{\mu_{rr}}{\mu_{zz}} = \frac{\kappa^2}{\nu^2} \frac{\langle a^2 \rangle}{\langle z_{\max}^2 \rangle} . \qquad (63)$$

Therefore, they do not keep a constant ratio, like that of Eq. (61). The ratio is proportional to the ratio of the mean squared amplitudes of the sample.

5.2. General case

In models that are more complex than the epicycle approximation, possible drifts along the other directions, similarly to the asymmetric drift for the rotation component of Eq. (56), are written as

$$\Delta_r = \Pi_c(S_0) - \Pi_0(S_0) ,$$
$$\Delta_z = Z_c(S_0) - Z_0(S_0) , \qquad (64)$$

although $\Pi_c(S_0) = Z_c(S_0) = 0$, we prefer to maintain such a notation. Nevertheless, for samples near the Galactic plane, these quantities generally vanish.

It is straightforward to estimate the ratio of the semiaxes of the velocity ellipsoid for a model without neglecting the asymmetric drift and the mean radial velocity. We rewrite Eqs. (42) and (46) as

$$(\Pi - \Pi_0) + (\Pi_0 - \Pi_c(S_0)) = \kappa a \cos(\kappa t - p) ,$$

$$(\Theta - \Theta_0) + (\Theta_0 - \Theta_c(S_0)) = -\kappa \gamma_c^{-1} a \sin(\kappa t - p) . \qquad (65)$$

By squaring those expressions and calculating their expected value, we get:

$$\mu_{rr} + (\Pi_0 - \Pi_c(S_0))^2 = \frac{1}{2} \kappa^2 \langle a^2 \rangle ,$$
$$\mu_{\theta\theta} + (\Theta_0 - \Theta_c(S_0))^2 = \frac{1}{2} \kappa^2 \gamma_c^{-2} \langle a^2 \rangle . \qquad (66)$$

41

Adding the foregoing equations and reordering terms, we get a general expression for Eq. (60):

$$\mu_{rr} + \gamma_c^2\,\mu_{\theta\theta} = \kappa^2\langle a^2\rangle - (\Pi_0 - \Pi_c)^2 - \gamma_c^2\,(\Theta_0 - \Theta_c)^2\ .\tag{67}$$

For the ratio, we get

$$\frac{\mu_{rr}}{\mu_{\theta\theta}} = \frac{\tfrac{1}{2}\kappa^2\langle a^2\rangle - (\Pi_0 - \Pi_c(S_0))^2}{\tfrac{1}{2}\kappa^2\gamma_c^{-2}\langle a^2\rangle - (\Theta_0 - \Theta_c(S_0))^2}\ .\tag{68}$$

This equation generalises that of Ninković (1992), where a vanishing radial mean velocity was assumed. Its right-hand side term depends on the average values of the sample and, in particular, would require a higher-order model to express the velocity differences in terms of the averaged amplitudes. This is left for a future work.

In particular, by using Eqs. (56) and (64), the expressions in Eq. (66) become

$$\mu_{rr} + \Delta_r^2 = \tfrac{1}{2}\kappa^2\langle a^2\rangle\ ,$$
$$\mu_{\theta\theta} + \Delta_\theta^2 = \tfrac{1}{2}\kappa^2\gamma_c^{-2}\langle a^2\rangle\ ,\tag{69}$$

so that the constant γ_c^2 accounts for something slightly different than the ratio of axes,

$$\frac{\mu_{rr} + \Delta_r^2}{\mu_{\theta\theta} + \Delta_\theta^2} = \gamma_c^2\ .\tag{70}$$

This expression is more realistic than Eq. (61). Since the asymmetric drift Δ_θ cannot be measured in terms of averaged eccentricities according the epicycle model, it must be estimated in an alternative way.

For the vertical motion, for stars with orbits far from circular, we can do a similar reasoning. Then, the corresponding equations can be written by using Eq. (64) as follows. For the vertical velocity distribution we have

$$\mu_{zz} + \Delta_z^2 = \frac{1}{2}\nu^2\langle z_{\max}^2\rangle\ ,\tag{71}$$

and, by combining the vertical and radial distributions, we have

$$\frac{\mu_{rr} + \Delta_r^2}{\mu_{zz} + \Delta_z^2} = \frac{\kappa^2}{\nu^2}\ \frac{\langle a^2\rangle}{\langle z_{\max}^2\rangle}\ .\tag{72}$$

Therefore, we find that the ratio in Eq. (70) should be maintained for different stellar subsamples, since it does not depend on the distribution of their eccentricities. Instead, the ratio in Eq. (72) depends on the distribution of the planar and vertical eccentricities, hence it is not constant for different stellar subsamples. In particular, for samples with $\Delta_r = \Delta_z = 0$, the ratio μ_{rr}/μ_{zz} is not necessarily the same.

6. APPROACH AND RESULTS

The current analysis can also be used to deduce the local kinematical constants from subsamples of the thin disc drawn from the GCSIII catalogue, selected with planar eccentricities $0 \leq e < 0.30$ and $z_{\max} \leq 0.5$ kpc (Cubarsi 2010). We will not repeat here the discussion about the sampling parameters, although we do point out that other sampling criteria like metalicity or Strömgren photometry such as $b - y$ colour were not able to describe the small-scale structure of the velocity distribution as eccentricities did (ibid. Figures 7 and 8). The eccentricities in the catalogue were recalculated in Stojanović (2015) and compared with those obtained by computing the star orbits by following the approach of Vidojević and Ninković (2009), resulting in a totally similar distribution.

For velocities, we now use a heliocentric coordinate system, with the radial heliocentric velocity component U positive towards the GC, the heliocentric velocity component V positive in the direction of the Galactic rotation, and the velocity component Z perpendicular to the Galactic plane and positive towards the NGP. The velocities (Π, Θ, Z) of previous Galactocentric coordinate system have the radial velocity component Π positive towards the Galactic anticentre and the other coordinates with similar orientation as the heliocentric system.

For several subsamples $\Sigma(e_0, z_0)$ of maximum eccentricity e_0 and maximum vertical amplitude z_0, the mean velocities, the central velocity moments[2], and the expected values $E(e)$, $E(e^2)$, $E(z_{\max})$, and $E(z_{\max}^2)$ were computed. They are shown in Table 1. Our purpose is to use the common trends of these nested subsamples to deduce the local constants. Instead, we do not intend to discuss whether a particular subsample is more kinematically representative of the local neighbourhood than the others.

6.1. Nested subsamples by eccentricity

For fixed $z_0 = 0.5$, we select a number of samples $\Sigma(e_0)$ for decreasing values of e_0. The lower the limit e_0, the lower the moments $\mu_{rr} \equiv \mu_{200}$ and $\mu_{\theta\theta} \equiv \mu_{020}$. This is the expected behaviour according to Eq. (59).

The subsamples $\Sigma(e_0)$ are used to estimate the factors $c_1 = \tfrac{1}{2}\kappa^2 r_0^2$ and $c_2 = \tfrac{1}{2}\kappa^2\gamma_c^{-2}r_0^2$ in Eq. (59). They allow to compute the local values for κ and γ_c^2 for each subsample listed in Table 1. While the values for κ derived from the sample moments μ_{200} are very stable, the values for Ω_c obtained through the fit of μ_{020} vary within about 30%, showing a decreasing trend as the eccentricity decreases. These values are fitted all together by using the least squares.

---

[2]We express the moments in the Greek indices notation, i.e., by making explicit the velocity powers, according to $\mu_{\alpha\beta\gamma} = \langle u_1^\alpha u_2^\beta u_3^\gamma\rangle$, depending on the peculiar velocity components.

Table 1. The columns in grey indicate the sampling parameters. Number of stars N, limiting eccentricity e_0, limiting height z_0 (kpc), several average values, mean heliocentric velocity components (km s^{-1}), and second central moments (km^2 s^{-2}) with their sampling variances are listed for each sample. For the samples selected by eccentricity, the resulting planar epicycle frequency (km s^{-1} kpc^{-1}) –it is assumed $r_c = 8.5$ kpc– and the ratio γ_c^2 of μ_{200} and μ_{020} are also listed. For samples selected by the maximum height, the resulting vertical epicycle frequency and the ratio of both frequencies are displayed.

N	e_0	$E(e)$	$E(e^2)$	z_0	$E(z_{max})$	$E(z_{max}^2)$	U_0	V_0	W_0	μ_{200}	μ_{110}	μ_{020}	μ_{101}	μ_{011}	μ_{002}	κ	γ_c^2
12056	0.29	0.105	0.014	0.50	0.162	0.038	-9.5 ± 0.26	-15.74 ± 0.16	-6.93 ± 0.11	843.28 ± 11.12	89.83 ± 4.85	325.5 ± 4.56	-1.67 ± 3.23	6.95 ± 2.12	135.33 ± 1.57	40.14	2.59
11119	0.20	0.0932	0.0109	0.50	0.159	0.037	-9.23 ± 0.24	-13.68 ± 0.15	-6.89 ± 0.11	653.02 ± 7.72	69.32 ± 3.57	247.82 ± 3.36	-0.69 ± 2.84	6.08 ± 1.86	130.94 ± 1.6	40.78	2.64
9719	0.15	0.0809	0.0078	0.50	0.156	0.036	-9.89 ± 0.22	-11.58 ± 0.14	-6.8 ± 0.11	489.66 ± 5.63	59.05 ± 2.61	178.77 ± 2.32	-2.06 ± 2.54	0.46 ± 1.65	126.93 ± 1.68	41.71	2.74
7170	0.10	0.0646	0.0048	0.50	0.152	0.034	-9.94 ± 0.2	-9.52 ± 0.13	-6.63 ± 0.13	278.28 ± 3.4	47.85 ± 1.84	130.57 ± 1.7	-2.77 ± 2.16	-4.2 ± 1.53	122.13 ± 1.92	40.13	2.13
2409	0.05	0.0355	0.0014	0.50	0.155	0.035	-9.62 ± 0.19	-5.97 ± 0.14	-6.96 ± 0.23	83.18 ± 1.73	6.38 ± 1.05	46.35 ± 1.01	1.83 ± 2.13	0.49 ± 1.62	128.6 ± 3.44	40.00	1.79
1052	0.03	0.0221	0.0006	0.50	0.146	0.031	-9.83 ± 0.18	-5.9 ± 0.13	-7.61 ± 0.33	33.48 ± 1.02	0.47 ± 0.6	17.17 ± 0.6	1.17 ± 1.9	-0.32 ± 1.48	116.93 ± 4.77	40.93	1.95
213	0.01	0.0089	0.0001	0.50	0.136	0.028	-10.32 ± 0.17	-5.55 ± 0.14	-7.04 ± 0.71	5.88 ± 0.43	0.03 ± 0.28	3.92 ± 0.28	-0.73 ± 1.6	-1.76 ± 1.59	107.09 ± 10.69	42.83	1.50

N	e_0	$E(e^2)$	z_0	$E(z_{max})$	$E(z_{max}^2)$	U_0	V_0	W_0	μ_{200}	μ_{110}	μ_{020}	μ_{101}	μ_{011}	μ_{002}	ν	ν/κ
12056	0.29	0.014	0.50	0.162	0.038	-9.5 ± 0.26	-15.74 ± 0.16	-6.93 ± 0.11	843.28 ± 11.12	89.83 ± 4.85	325.5 ± 4.56	-1.67 ± 3.23	6.95 ± 2.12	135.33 ± 1.57	84.12	2.10
9793	0.29	0.014	0.25	0.119	0.018	-9.62 ± 0.29	-15.72 ± 0.17	-7.25 ± 0.08	801.81 ± 11.73	92.3 ± 5.08	298.18 ± 4.65	-6.28 ± 2.38	4.32 ± 1.46	65.76 ± 0.69	84.79	2.11
8574	0.29	0.013	0.20	0.104	0.013	-9.83 ± 0.3	-15.67 ± 0.18	-7.31 ± 0.07	771.88 ± 12.09	93.26 ± 5.24	291.91 ± 4.87	-4.94 ± 2.06	4.67 ± 1.29	46.89 ± 0.51	83.56	2.09
6832	0.29	0.013	0.15	0.085	0.009	-10.39 ± 0.33	-15.57 ± 0.2	-7.24 ± 0.06	746.55 ± 13.08	94.29 ± 5.72	283.01 ± 5.44	-2.24 ± 1.75	3.9 ± 1.09	28.76 ± 0.34	81.48	2.04
4540	0.29	0.013	0.10	0.062	0.005	-10.74 ± 0.4	-15.59 ± 0.25	-7.18 ± 0.06	732.88 ± 15.83	101.82 ± 6.91	280.02 ± 6.63	-3.9 ± 1.46	-1.03 ± 0.92	14.04 ± 0.2	78.24	1.96
2824	0.29	0.013	0.07	0.046	0.002	-10.73 ± 0.51	-15.42 ± 0.31	-7.11 ± 0.05	726.48 ± 20.76	102.36 ± 8.61	273.3 ± 8.37	-1.79 ± 1.27	-1.1 ± 0.79	6.86 ± 0.13	75.38	1.88
1823	0.29	0.013	0.05	0.035	0.001	-10.96 ± 0.63	-15.29 ± 0.39	-7.15 ± 0.05	733.1 ± 26.68	110.26 ± 10.9	274.52 ± 10.38	-2.23 ± 1.15	-0.77 ± 0.74	3.8 ± 0.09	73.31	1.83

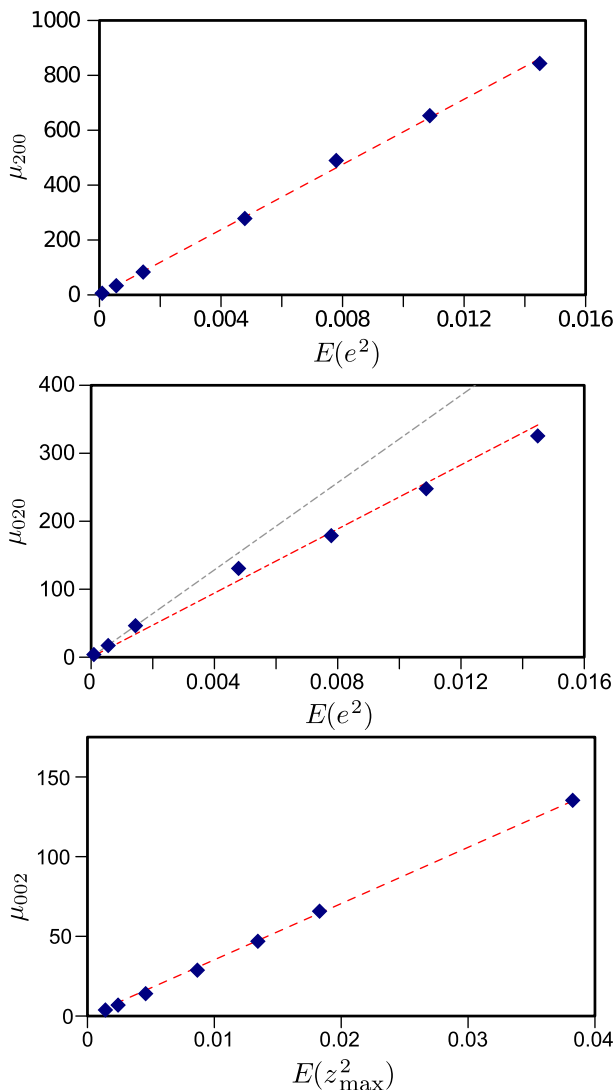**Fig. 2.** *Diagonal second central moments (km² s⁻²) (blue diamonds) in terms of the average squared eccentricities of the samples. The upper and middle panel are for samples selected by planar eccentricity, the bottom panel is for samples selected by maximum height. Regression lines are plotted as red dashed lines. For the middle panel, the grey dashed line fits the three samples with lower e_0. (See the electronic edition of the Journal for a color version of this figure).*

The corresponding regression lines are shown in the upper and middle panel of Fig. 2. The fit for μ_{200} (red dashed line) is very accurate and yields $\kappa = 41.1 \pm 0.2$ km s⁻¹kpc⁻¹. However, the regression line for μ_{020} is not good enough. In the middle panel, the grey dashed line also fits the three samples with the lowest eccentricity $e_0 = 0.01, 0.03, 0.05$, that show a more similar trend. Note that the weight on the overall resulting slope of the samples with lower eccentricities is lower, since the least squares fit must contain the origin. Therefore, the resulting Ω_c from the fit is not obtained as an average of values ob-

tained from single samples. This has another consequence: although the sampling errors of moments of samples with lower eccentricities and fewer stars are higher, there is a discrepancy in the slope of the two lines.

As explained in the previous section, the missed term of the asymmetric drift is responsible for this less accurate fitting. According to Strömgren's law, the asymmetric drift is lower for populations with lower moment μ_{rr}. Then, the better estimation of Ω_c according to Eq. (61) is obtained from the lower eccentricity samples that have fewer stars and greater uncertainty in their estimates.

This means that the second term in Eq. (59) should be interpreted as

$$\frac{1}{2}\kappa^2\gamma_c^{-2} = \lim_{a \to 0} \frac{\mu_{\theta\theta}}{\langle a^2 \rangle} , \qquad (73)$$

provided the sample has enough stars for the moment to be significant. Otherwise, the asymmetric drift must be taken into account.

In such a case, we label the peculiar velocity of the Sun as $(u_\odot, v_\odot, w_\odot) = (\Pi_\odot - \Pi_c, \Theta_\odot - \Theta_c, Z_\odot - Z_c)$ and the heliocentric mean velocity of the sample as $(U_0, V_0, W_0) = (\Pi_0 - \Pi_\odot, \Theta_0 - \Theta_\odot, Z_0 - Z_\odot)$. Then, the asymmetric drift may be expressed as $\Delta = \Theta_c - \Theta_0 = -v_\odot - V_0$.

For these samples we estimate the asymmetric drift according to Strömgren's classical law

$$\Delta = -v_\odot - V_0 = k\,\mu_{rr} ,$$

with k constant. In the top panel in Fig. 3 it is adjusted in the form

$$V_0 = -v_\odot - k\,\mu_{rr} .$$

This provides values $v_\odot = 5.25 \pm 0.31$ km s⁻¹ and $k = 0.0325 \pm 0.0016$ km⁻¹s.

We also check the new Strömgren's non-linear relation (Golubov et al. 2013)

$$\Delta' = -\frac{\mu_{rr} + \eta(\mu_{rr} - \mu_{zz}) - \mu_{\theta\theta} - V_0^2}{2\Theta_\odot} - \frac{v_\odot^2}{2\Theta_\odot} + k'\,\mu_{rr} ,$$

with $\eta = 1$ which takes into account the ratio between the axes of the velocity ellipsoid. The first term on the right-hand side depends on the sample, while the second one is constant. In this case, the resulting peculiar rotation velocity of the Sun is slightly lower, although within the error margin of the above value. Therefore, for these samples it provides a similar estimation. For both cases, the asymmetrical drift is depicted in the middle panel in Fig. 3.

The estimation of the local angular velocity obtained for the three samples with lower eccentricities, so to say according to Eq. (73), is $\Omega_c = 28.4 \pm 0.4$ km s⁻¹kpc⁻¹ corresponding to the grey straight line in the bottom panel in Fig. 3. We assumed $r_c = 8.5$ kpc as we did for the values of Table 1. Notice that the value Ω_c obtained from these three small samples by the least squares estimation forcing to intercept by zero is much better than the average of the angular velocity of the samples.
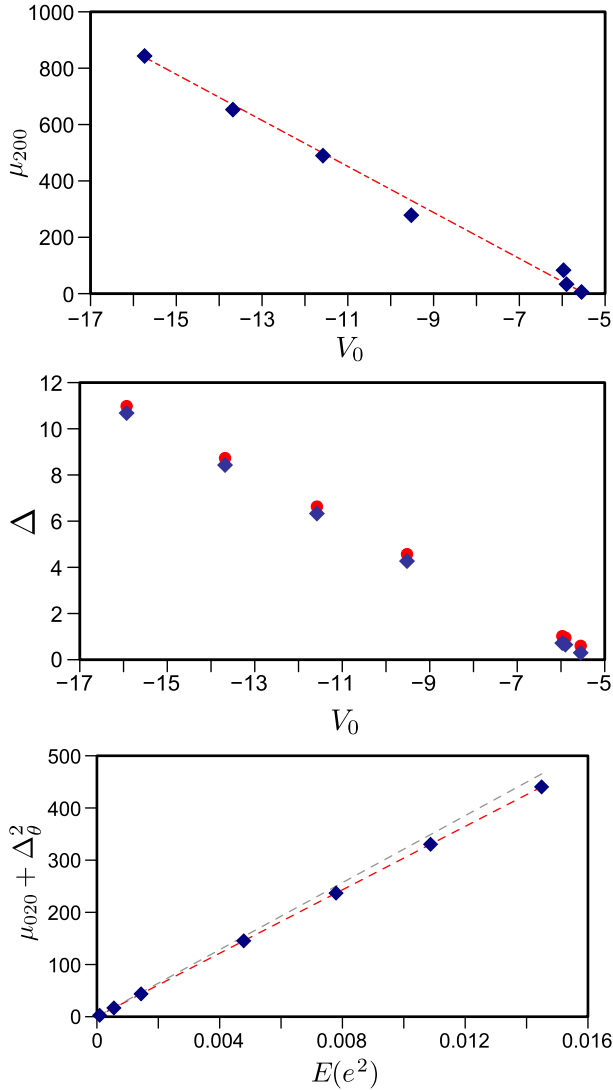
$$\Delta^2 = \gamma_{\rm c}^{-2}\mu_{rr} - \mu_{\theta\theta} \; , \qquad (74)$$

provided the local constants are known.

6.2. Nested subsamples by maximum height

Now we fix the value for e_0 and select a set of nested subsamples $\Sigma(z_0)$ with decreasing z_0. For these samples, the lower z_0, the lower $\mu_{zz} \equiv \mu_{002}$. This was predicted by Eq. (62). However, the ratio μ_{200}/μ_{020} remains nearly constant for all the subsamples. For instance, if the subsample selected by $e_0 = 0.05$ and $z_0 = 0.5$ kpc in Table 1 is now limited to $z_0 = 0.3$, the moments μ_{200} and μ_{020} do not change but we get the moment $\mu_{002} = 81.15 \pm 1.98$ km^2 s^{-2} which is 63% lower. This fact should be taken into account in selecting samples to study the velocity distribution. Nevertheless, the local values derived from both subsamples i.e. the epicycle frequencies and the angular velocity, are significantly maintained. In addition, from Table 1 we see that the mean value $E(e)$ also remains nearly constant. The least squares fitting of Eq. (62) (Fig. 2, bottom panel) provides the vertical epicycle frequency with good accuracy, $\nu = 84.0 \pm 0.4$ km s^{-1}kpc^{-1}.

Fig. 3. *(Top) Strömgren's law relating the second velocity moments (km^2 s^{-2}) to the heliocentric mean velocities (km s^{-1}) of the subsamples. (Middle) Asymmetric drift (km s^{-1}) according to Strömgren's classical law (blue diamonds) and the new relation (red circles). (Bottom) Fitting the second expression of Eq. (69). The grey dashed line is the fit of the three samples with lower e_0, and the red one is the least squares approximation for all the samples. (See the electronic edition of the Journal for a color version of this figure).*

By taking into account the asymmetric drift i.e. from the second expression of Eq. (69), we get $\Omega_{\rm c} = 29.2 \pm 0.4$ km s^{-1}kpc^{-1}. It corresponds to the red line fit in the bottom panel in Fig. 3. If the local radius is taken as $r_{\rm c} = 8$ kpc, we get $\Omega_{\rm c} = 27.4 \pm 0.4$ km s^{-1}kpc^{-1}, which is totally consistent with the usually assumed value.

Therefore, the asymmetric drift of the stars in the sample can be estimated as
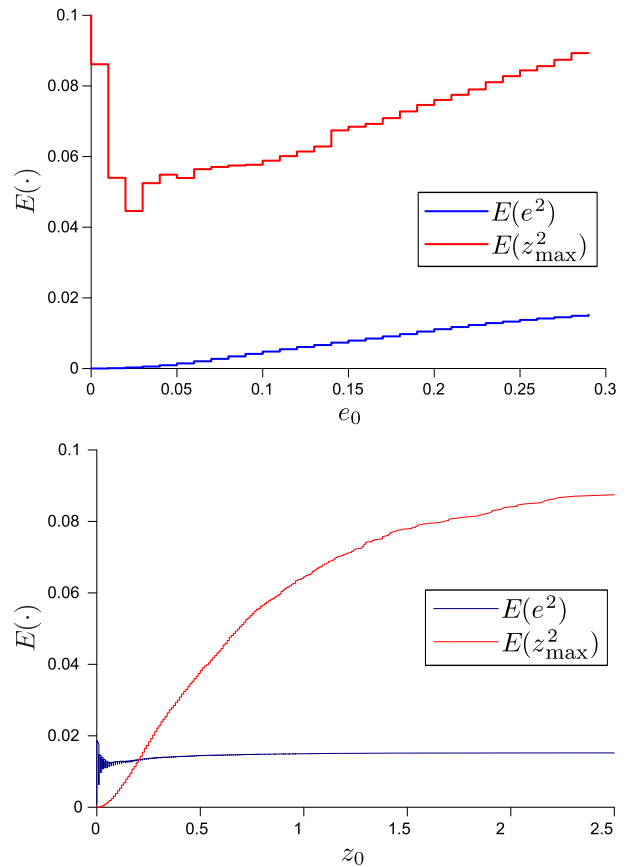

Fig. 4. *Average values of e and $z_{\max}$ for samples limited by eccentricity e_0 or maximum height z_0. (See the electronic edition of the Journal for a color version of this figure).*

Indeed, the planar and the vertical amplitudes are not totally independent. In terms of the mean square eccentricity and maximum height, this behaviour is shown in Fig. 4 for the whole GCSIII sample with $0 \leq e < 0.30$, but without limiting $z_{\max}$ (13000 stars in total). The first graph shows the average $E(z_{\max}^2)$ (in red) in terms of the limiting eccentricity e_0. It is a monotonous increasing function for $e_0 \geq 0.03$, growing simultaneously with $E(e^2)$ (in blue). This fact should be taken into account specially when working with samples of lower planar eccentricity, since a kinematically representative sample should not contain many stars with high values of $z_{\max}$. However, the second graph shows that $E(e^2)$ is independent from z_0 (blue line).

Therefore, for a sample $\Sigma(e_0)$ the approximate value z_0 for its maximum height can be determined in the following way. The first graph provides the average $E(z_{\max}^2)$ in terms of the limit eccentricity e_0. Then, the second graph for the average $E(z_{\max}^2)$ in terms of z_0, read backwards, gives the approximate limit z_0. For samples obtained from the limit z_0 the procedure cannot be applied, since $E(e^2)$ in terms of z_0 is almost constant.

For instance, a subsample selected by $e_0 = 0.1$, according to the first graph of Fig. 4 has $E(z_{\max}^2) \approx 0.06$. The second graph tell us that this value corresponds to a sample limited by $z_0 \approx 1$ which means that we should not include stars with $z_{\max} > 1$. For a limiting value $e_0 = 0.03$, which is the lower limit of this definite trend shown by the first graph, we estimate $E(z_{\max}^2)$ between 0.04 and 0.5. This average value read in the second graph tells us that in the sample we should not include stars with $z_{\max}$ higher than 0.5 or 0.6.

This was a reasoning based on experimental facts that should be further investigated i.e. how the limits e_0 and z_0 are constrained. However, since the epicycle model addresses the vertical and planar motions in an independent way, it does not provide a direct solution.

6.3. The simplest potential

According to the actual values of the local constants, the potential can be none of the two particular cases of Eq. (2) and Eq. (23), neither separable in cylindrical coordinates nor spherical. The former case provides a ratio between the epicycle frequencies $\kappa/\nu = 2$ and the latter leads to $\nu^2 = \Omega_{\rm c}^2$, both unrealistic. We then study the general case of Eq. (1). In the Galactic plane, such a potential becomes very simple. It has a term proportional to r^2 and another proportional to r^{-2}.

To discuss the values of the local constants we propose a simple case example consisting in a modification of the spherical potential,

$$\mathcal{U} = M\,(r^2 + z^2) + \frac{N}{r^2 + Q z^2} \, , \qquad (75)$$

that is, with

$$F(s) = N\,(1 + Q\,s)^{-1} \, ,$$

in Eq. (1) with N, Q are constant. It could be said that this is the simplest quasi-stationary potential allowing to estimate the three constants in an independent way. We prefer to interpret it as a slight deviation of the spherical potential instead of using the nearly equivalent potential (for small values of s) with $F(s) = N\,(1 - Q\,s)$ i.e. a first degree polynomial taken from the power series of $F(s)$. Then, we have $F(0) = N$ and $F'(0) = -NQ$ from where we determine the constants M, N, and the dimensionless constant Q involved in the potential as

$$M = \frac{1}{8}\kappa^2 \, ,$$

$$N = \frac{r_{\rm c}^4}{2}\left(\frac{\kappa^2}{4} - \Omega_{\rm c}^2(r_{\rm c})\right) \, ,$$

$$Q = \frac{4\nu^2 - \kappa^2}{4\Omega_{\rm c}^2(r_{\rm c}) - \kappa^2} \, .$$

Thus, $Q = 0$ corresponds to the cylindrical potential and $Q = 1$ to the spherical potential.
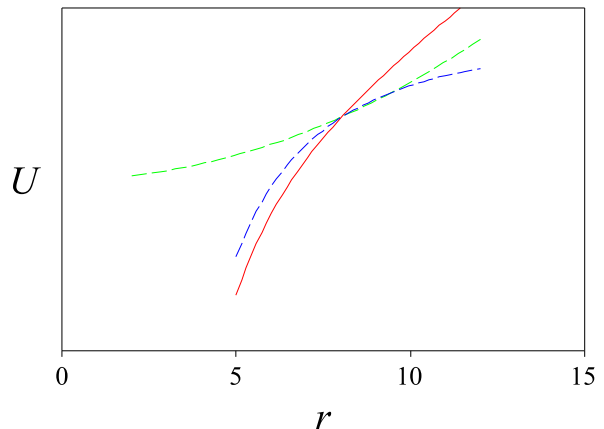

Fig. 5. *Local behaviour of the potential of Eq. (75) (red continuous line) compared with the harmonic potential (green dashed line) with $N = 0$, and with the potential with $M = 0$ (blue dashed line) without the harmonic term. (See the electronic edition of the Journal for a color version of this figure).*

For the local constants, this yields $Q \approx 11.7$, which means that the term $\frac{1}{r^2}F(\frac{z^2}{r^2}) = \frac{N}{r^2 + Q z^2}$ will have elliptical isocontours $(\frac{r}{\sqrt{Q}})^2 + z^2 = \mathrm{const}$ with $\sqrt{Q} = 3.4$. We also compare in Fig. 5 the local behaviour of such a potential (in red) at $r_{\rm c}$ in the symmetry plane with that of a potential with $N = 0$ i.e. the harmonic potential (in green), and with a potential with $M = 0$ (in blue) i.e. only with the term proportional to r^{-2}. It is clear that both terms have a significant contribution to the shape of the local potential.

7. DISCUSSION

The selection of nested disc subsamples drawn from the GCSIII catalogue by using as sampling parameters the planar and vertical eccentricities is particularly useful to determine the three Galactic constants related to the first derivatives of the potential at the solar position, namely, the two epicycle frequencies and the local angular velocity. The first-order epicycle model accurately describes the relationships between the mean squared planar and vertical eccentricities of the subsamples and their velocity moments μ_{rr} and μ_{zz}, which are linearly constrained through the respective planar and vertical epicycle frequencies. However, this model is unable to provide a similar relationship involving the mean squared planar eccentricity and the moment $\mu_{\theta\theta}$, which should provide the local angular velocity Ω_c. This can be addressed by taking into account the asymmetric drift of the subsamples, estimated from Strömberg's law or from its non linear improvement. Therefore, Eq. (74) provides a way to estimate the asymmetric drift in terms of the second velocity moments.

The current eccentricity samples yield actual values obtained from kinematically selected samples (e.g. Dehnen 1998) for the planar and vertical epicycle frequencies $\kappa = 41.1 \pm 0.2$ km s^{-1}kpc^{-1} and $\nu = 84.0 \pm 0.4$ km s^{-1}kpc^{-1}. The local angular velocity was estimated as $\Omega_c = 29.2 \pm 0.4$ km s^{-1}kpc^{-1} for $r_c = 8.5$ kpc. The ratio Ω_c/κ yields a 3/4 resonance between the radial and azimuthal orbital frequencies. As we see, the samples selected by planar eccentricity are very similar, as for the radial and vertical mean velocity components they tend towards values $\Pi_0 = 10$ km s^{-1} and $Z_0 = -7$ km s^{-1}, respectively. Neither the samples limited by very low eccentricities are an exception. Therefore, it is possible to conclude that the stars belonging to such samples do move along almost circular orbits; in favour is the trend of decreasing dispersion. As a consequence, a value of $v_\odot = 5.25 \pm 0.31$ km s^{-1} seems acceptable for the rotational component of the solar motion. Nevertheless, these values may differ from those obtained from velocity distributions reflecting chemodynamical properties, such as Schönrich et al. (2010) who, by using the same GCS catalogue, although introducing a selection criterion based on metalicities, obtained estimates corresponding to our samples with maximum eccentricity within the range $0.15 < e_0 < 0.20$.

It is also noticeable that the ratio $\mu_{rr}/\mu_{\theta\theta}$ tends to be smaller as the eccentricities are lower. With regard to our interpretation this is expectable because in the case of extremely low eccentricities the asymmetric drift is negligible, but not for higher eccentricities. In this way one can explain why the classical formula of Eq. (61) leads to values of about 1.6 for the ratio $\frac{A}{|B|} = \text{sign}(\gamma_c)(\gamma_c^2 - 1)$. This value is artificially increased because the asymmetric drift Δ is neglected. Nevertheless, for samples limited by $e_0 < 0.3$ its square is about $\Delta^2 = 110$ km^2 s^{-2}, which is not negligible. Once the asymmetric drift is taken into account, we obtain a ratio $\gamma_c = \frac{2\Omega_c}{\kappa} = 1.42$ that provides a quotient $\frac{A}{|B|} = 1.02$. In other words, ratios $\mu_{rr}/\mu_{\theta\theta} \approx 2.6$ can agree with $\frac{A}{|B|} \approx 1$ suggested by the rotation curves.

Therefore, this leaves open how to model the asymmetric drift or, more general, how to express motions relative to the local standard of rest in Eq. (66) in terms of the averaged planar eccentricity of the subsamples. In such a case, a higher-order epicycle model will be needed.

To study how the Galactic constants constrain the potential in the solar neighbourhood, we have adopted a quasi-stationary potential function (Cubarsi 2014a, 2014b). This potential, which is axisymmetric although valid for point-axially symmetric stellar systems as well, is the solution of the time-dependent Boltzmann collisionless equation when the velocity distribution is a mixture of ellipsoidal populations with arbitrary mean velocity components and arbitrary orientation of the velocity ellipsoid.

For disc stars, showing a more complex velocity distribution than the halo stellar samples used to test the spherical symmetry of the potential, we have proved that the potential cannot be separable in addition in cylindrical coordinates and cannot be spherically symmetric. In particular, it has been argued in terms of main trends of the velocity distribution such as the velocity dispersions and the asymmetric drift which are related to the local values of the epicycle frequencies and the local angular velocity, without the need of discussing more detailed features of the velocity distribution, such as the vertex deviation or the radial mean velocity of the samples, which, on the other hand, are consistent with this type of potential.

REFERENCES

An, J. and Evans, N. W.: 2016, *Astrophys. J.*, **816**, 35.
Arnold, V. I.: 1989, Mathematical methods of classical mechanics, Springer-Verlag, New York.
Binney, J. and Tremaine, S.: 2008, Galactic Dynamics (Second edition), Princeton University Press, Princeton.
Carollo, D. et al.: 2010, *Astrophys. J.*, **712**, 692.
Casetti-Dinescu, D.I., Girard, T.M., Korchagin, V.I. and van Altena, W.F.: 2011, *Astrophys. J.*, **728**, 7.
Chandrasekhar, S.: 1960, Principles of Stellar Dynamics, Dover Publications Inc., New York.
Cubarsi, R.: 2010 *Astron. Astrophys.*, **510**, A103.
Cubarsi, R., Alcobé, S., Vidojević, S. and Ninković, S.: 2010, *Astron. Astrophys.*, **510A**, 102.
Cubarsi, R.: 2014a, *Astron. Astrophys.*, **561**, A141.
Cubarsi, R.: 2014b, *Astron. Astrophys.*, **567**, A46.

Dehnen, W.: 1998, *Astron. J.*, **115**, 2384.

Eddington, A.S.: 1915, *Mon. Not. R. Astron. Soc.*, **76**, 37.

Evans, N. W., Sanders, J. L., Williams, A. A., An, J., Lynden-Bell, D. and Dehnen, W.: 2016, *Mon. Not. R. Astron. Soc.*, **456**, 4506.

Fuchs, B. et al.: 2009, *Astron. J.*, **137**, 4149.

Golubov, O. et al.: 2013, *Astron. Astrophys.*, **557**, A92.

Holmberg, J., Nordström, B. and Andersen, J.: 2007, *Astron. Astrophys.*, **475**, 519.

Holmberg, J., Nordström, B. and Andersen, J.: 2009, *Astron. Astrophys.*, **501**, 941.

Lynden-Bell, D.: 1962, *Mon. Not. R. Astron. Soc.*, **124**, 95.

Moni Bidin, C., Carraro, G. and Méndez, R.A.: 2012, *Astrophys. J.*, **747**, 101.

Ninković, S.: 1992, *Astrophys. Space Sci.*, **187**, 159.

Ninković, S.: 2009, *Serb. Astron. J.*, **179**, 49.

Ninković, S.: 2011, *Astrophysics*, **54**, 439.

Nordström, B. et al.: 2004, *Astron. Astrophys.*, **418**, 989.

Pasetto, S. et al.: 2012a, *Astron. Astrophys.*, **547**, A70.

Pasetto, S. et al.: 2012b, *Astron. Astrophys.*, **547**, A71.

Sala, F.: 1990, *Astron. Astrophys.*, **235**, 85.

Schönrich, R., Binney, J. and Dehnen, W.: 2010, *Mon. Not. R. Astron. Soc.*, **403**, 1829.

Siebert, A. et al.: 2008, *Mon. Not. R. Astron. Soc.*, **391**, 793.

Smith, M. C., Wyn Evans, N. and An, J. H.: 2009a, *Astrophys. J.*, **698**, 1110.

Smith, M. C. et al.: 2009b, *Mon. Not. R. Astron. Soc.*, **399**, 1223.

Steinmetz, M.: 2012, *Astron. Nachr.*, **333**, 523.

Stojanović, M.: 2015, *Serb. Astron. J.*, **191**, 75.

Vidojević, S. and Ninković, S.: 2009, *Astron. Nachr.*, **330**, 46.

APPENDIX

A. Epicycle approximation

In absence of collisions, the motion of a star in a galaxy is derived from a gravitational potential $\mathcal{U}$, generally assumed to be stationary. In a cylindrical coordinates system, if we mark the star position as (r, θ, z) and the velocity of the star as $(\Pi, \Theta, Z) = (\dot{r}, r\dot{\theta}, \dot{z})$, the equations of motion may be written as

$$\frac{d^2 r}{dt^2} = r\dot{\theta}^2 - \frac{\partial \mathcal{U}}{\partial r} \ ,$$

$$\frac{d}{dt}(r^2 \dot{\theta}) = -\frac{\partial \mathcal{U}}{\partial \theta} \ , \qquad (76)$$

$$\frac{d^2 z}{dt^2} = -\frac{\partial \mathcal{U}}{\partial z} \ .$$

Two isolating integrals of motion exist for all orbits under steady-state and axisymmetric potentials. That is

$$\frac{\partial \mathcal{U}}{\partial t} = \frac{\partial \mathcal{U}}{\partial \theta} = 0 \ . \qquad (77)$$

One is the energy integral

$$I = \Pi^2 + \Theta^2 + Z^2 + 2\mathcal{U}(r, z) \ , \qquad (78)$$

and the other one is the axial component of the angular momentum

$$J = r\Theta = r^2 \dot{\theta} \ . \qquad (79)$$

For a fixed integral of motion J, the energy integral may be written as

$$I = \Pi^2 + Z^2 + 2\mathcal{V}(r, z); \quad \mathcal{V}(r, z) = \frac{J^2}{2r^2} + \mathcal{U}(r, z) \ , \qquad (80)$$

where $\mathcal{V}(r, z)$ is the *effective potential energy*.

A third integral of motion, the so-called Oort's integral, exists if a separable potential $\mathcal{U} = \mathcal{U}_1(r) + \mathcal{U}_2(z)$ is assumed. It is valid near the Galactic plane. However, to our purposes, we shall only assume a less restrictive hypothesis: a Galactic plane of symmetry, $z = 0$. Thus, the potential satisfies

$$\left.\frac{\partial \mathcal{U}}{\partial z}\right|_{z=0} = 0 \ , \qquad (81)$$

which is equivalent to saying that $\mathcal{U}$ is a function even of z.

Let us assume a star moving in a stable orbit on the Galactic plane $z = 0$ with a vertical velocity component $\dot{z} = 0$. The third equation of Eq. (76), combined with Eq. (81), tells us that there is no acceleration in the vertical direction. Therefore, the motion of this star is restricted to the Galactic plane. We now fix the integral value J. By taking into account the energy integral of Eq. (80) we have

$$I = \dot{r}^2 + 2\mathcal{V}(r, 0) \ . \qquad (82)$$

Therefore, for each value of the energy integral I, the orbits, and, in particular, the values of r are constrained by the condition

$$\mathcal{V}(r, 0) \leq \frac{1}{2} I \ .$$

In general, the equation $\mathcal{V}(r, 0) = \frac{1}{2} I$ provides the extreme values of r for which $\dot{r} = 0$, by delimiting a annular region $r_{\min} \leq r \leq r_{\max}$ where the motion takes place (e.g. Arnold 1989, p35). In particular, by diminishing the value of I we reach a minimum value $I = I_c$, for which the epicentre and the apocentre coincide, say $r_c \equiv r_{\min} = r_{\max}$.

In this case the orbit becomes circular, and satisfies $r = r_c$, $\dot{r} = 0$ where r_c is a local minimum satisfying

$$\left.\frac{\partial \mathcal{V}(r, 0)}{\partial r}\right|_{r_c} = 0 \ , \qquad (83)$$

under the condition

$$\left.\frac{\partial^2 \mathcal{V}(r, 0)}{\partial r^2}\right|_{r_c} > 0 \ . \qquad (84)$$

To integrate the equations of motion for a circular orbit at radius $r = r_c$ with no radial acceleration, we make use of the angular momentum integral Eq. (79) in the first expression of Eq. (76), and take into account the relation

$$\frac{\partial \mathcal{V}}{\partial r} = -\frac{J^2}{r^3} + \frac{\partial \mathcal{U}}{\partial r} \; . \tag{85}$$

Then, by introducing the condition given by Eq. (83) we get

$$\ddot{r} = -\frac{\partial \mathcal{V}(r,0)}{\partial r}\bigg|_{r_c} = 0 \; . \tag{86}$$

Therefore, according to Eq. (85), for a star in circular motion in the plane $z = 0$ with angular momentum integral $J = J_c$, the radius r_c is obtained from the equality

$$\frac{\partial \mathcal{U}(r,0)}{\partial r}\bigg|_{r_c} = \frac{J_c^2}{r_c^3} \; . \tag{87}$$

The condition of minimum of Eq. (84) is now given, by taking into account Eq. (87), as[3]

$$\frac{\partial^2 \mathcal{V}(r,0)}{\partial r^2}\bigg|_{r_c} = \left(\frac{3}{r}\frac{\partial \mathcal{U}(r,0)}{\partial r} + \frac{\partial^2 \mathcal{U}(r,0)}{\partial r^2}\right)_{r_c} \equiv \kappa^2 > 0 \; . \tag{88}$$

The angular and circular velocities are constant, such that

$$\dot{\theta}_c \equiv \Omega_c = \frac{J_c}{r_c^2}; \quad \Theta_c = \frac{J_c}{r_c} \; . \tag{89}$$

According to Eq. (87) and Eq. (89), the value of the angular velocity is related to local properties of the potential as follows

$$\Omega_c^2 = \frac{1}{r_c}\frac{\partial \mathcal{U}(r,0)}{\partial r}\bigg|_{r_c} \; . \tag{90}$$

Thus, an orbit in the Galactic plane with circular motion and constant angular velocity corresponds to a local minimum value of the energy integral

$$I_c = \frac{J_c^2}{r_c^2} + 2\mathcal{U}(r_c, 0) \; , \tag{91}$$

and other orbits with the same angular momentum integral J_c are non-circular and have $I > I_c$ energy integral.

B. Oort constants

As well known, the constants are defined as

$$A = \frac{1}{2}\left(\frac{\Theta_c}{r} - \frac{\partial \Theta_c}{\partial r}\right)_{S_0} \; , \; B = -\frac{1}{2}\left(\frac{\Theta_c}{r} + \frac{\partial \Theta_c}{\partial r}\right)_{S_0} \; , \tag{92}$$

or, alternatively, they are used as a way of expressing the quantities

$$\Omega_c(S_0) = A - B, \quad \frac{\partial \Theta_c}{\partial r}\bigg|_{S_0} = -(A + B) \; . \tag{93}$$

Then, according to Eqs. (17) and (36), we have

$$\kappa^2 = 4B(B - A), \quad \gamma_c^2 = \frac{B - A}{B}, \quad \kappa \gamma_c^{-1} = -2B \; , \tag{94}$$

hence, the signs of B and $(B - A)$ are the same. Moreover, since the epicycle frequency is positive, B and $B - A$ have the opposite sign than γ_c.

Similarly, Oort's constants at S_0 can be approximated from local values of Ω_c, κ, and γ_c at S. Thus, we have

$$B \approx -\gamma_c^{-2}\,\Omega_c(S) \; , \quad A - B \approx \Omega_c(S) \; . \tag{95}$$

Therefore, the sign of $\Omega_c(S)$ is the same as γ_c and opposite to B.

In addition, since

$$A = \frac{\kappa}{2\gamma_c}(\gamma_c^2 - 1), \; |B| = \frac{\kappa}{2|\gamma_c|}, \; \frac{A}{|B|} = \frac{\gamma_c}{|\gamma_c|}(\gamma_c^2 - 1) \; ,$$

we get

$$\mathrm{sign}(A) = \mathrm{sign}\left(\frac{A}{|B|}\right) = \mathrm{sign}(\gamma_c)\,\mathrm{sign}(\gamma_c^2 - 1) \; .$$

In order to compute the star eccentricity, one approach (Stojanović 2015) is to approximate locally the circular velocity by a power law. Then, by writing

$$\Theta_c(r) = cr^\beta \tag{96}$$

owing to Eq. (93), we get the equivalences

$$\frac{A}{B} = \frac{\beta - 1}{\beta + 1}, \quad \beta = \frac{B + A}{B - A} = \frac{2 - \gamma_c^2}{\gamma_c^2} \; . \tag{97}$$

---

[3]This condition of stability of the orbit is equivalent to $\frac{1}{r^3}\frac{\partial}{\partial r} r^3 \frac{\partial \mathcal{U}(r,0)}{\partial r}\big|_{r_c} \equiv \kappa^2 > 0$, which can be used when the gravitational force is locally approximated by a power law i.e. $-\frac{\partial \mathcal{U}(r)}{\partial r} \approx -k^2 r^\alpha$, so that the condition implies $\alpha > -3$ to be fulfilled at the radius of a stable circular orbit.

On the other hand, to approximate the circular velocity in this way is also equivalent to approximating the gravitational force by a power law. Thus, similarly to the footnote of Eq. (88) where the stability of circular orbits is discussed, we write $\frac{\partial \mathcal{U}(r)}{\partial r} = kr^{\alpha}$. Then, from Eq. (34) we get $\Theta_{\mathrm{c}}(r) = kr^{\frac{\alpha+1}{2}}$. Therefore,

$$\alpha = 2\beta - 1 = \frac{4 - 3\gamma_{\mathrm{c}}^2}{\gamma_{\mathrm{c}}^2} \ . \qquad (98)$$

Only values $\alpha > -3$ provide us with stable orbits, which now correspond to values $\beta > -1$.

УЗОРЦИ ПО ЕКСЦЕНТРИЧНОСТИ: ИМПЛИКАЦИЈЕ ЗА ПОТЕНЦИЈАЛ И РАСПОДЕЛУ БРЗИНЕ

R. Cubarsi[1], M. Stojanović[2] and S. Ninković[2]

[1]*Departament de Matemàtiques, Universitat Politècnica de Catalunya, Barcelona, Spain*

E–mail: *rafael.cubarsi@upc.edu*

[2]*Astronomical Observatory, Volgina 7, 11060 Belgrade 38, Serbia*

E–mail: *mstojanovic@aob.rs, sninkovic@aob.rs*

Епицикличне учестаности у равни Млечног пута и нормално на њу и угаона брзина за Сунчев положај су повезане са потенцијалом за исти положај до његових извода другог реда и могу да се употребе за испитивање облика потенцијала на основу узорака сачињених од звезда диска. Пошто ови узорци показују сложенију расподелу брзине од звезда халоа, испитивање засновано на њима треба да буде реалније. Ми усвајамо обртно симетрични потенцијал који допушта мешавину независних елипсоидних расподела брзине чији је облик сепарабилан или Штекелов у цилиндричним или сферним координатама. Доказујемо да вредности локалних константи нису у сагласности са потенцијалом који је сепарабилан или сферно симетричан. Користимо најједноставнији потенцијал, у складу са локалним константама, да покажемо да су хармонијски и нехармонијски чланови потенцијала подједнако важни. Иста анализа се користи за процену вредности локалних константи. Две фамилије хијерархијских подузорака одабране у смеру смањивања ексцентричности за кретање у равни и ексцентричности по нормали на њу се користе ради добијања релације између средњих квадрата ексцентричности у равни и нормално на раван и дисперзија брзине у подузорцима. Према епицикличном моделу првог реда компоненте брзине дуж радијуса и нормале пружају коректну информацију о епицикличним учестаностима у равни и нормално на њу. Међутим, асиметрични дрифт не може да се објасни и настаје систематско померање у процени треће константе. У оквиру општијег модела, када се узима у обзир асиметрични дрифт, дисперзије брзине ротације заједно са својим разликама дају добро слагање у вези угаоне брзине за положај Сунца. Сагласност резултата показује да овај нови метод заснован на расподели ексцентричности треба да се користи у проучавању звездане кинематике.